

# A Dendritic Model of Coincidence Detection in the Avian Brainstem

Jonathan Z. Simon<sup>1</sup>  
Catherine E. Carr<sup>2</sup>  
Shihab A. Shamma<sup>1,3</sup>

<sup>1</sup>Institute for Systems Research

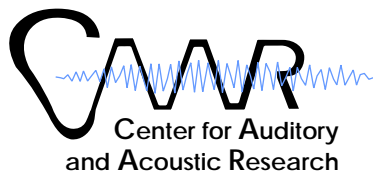
<sup>2</sup>Department of Biology

<sup>3</sup>Department of Electrical Engineering

University of Maryland

Supported in part by  
Office of Naval Research MURI grant N00014-97-1-0501  
and National Science Foundation grant 9720334

This poster is available at <<http://www.isr.umd.edu/CAAR/pubs.html>>



# Report Documentation Page

Form Approved  
OMB No. 0704-0188

Public reporting burden for the collection of information is estimated to average 1 hour per response, including the time for reviewing instructions, searching existing data sources, gathering and maintaining the data needed, and completing and reviewing the collection of information. Send comments regarding this burden estimate or any other aspect of this collection of information, including suggestions for reducing this burden, to Washington Headquarters Services, Directorate for Information Operations and Reports, 1215 Jefferson Davis Highway, Suite 1204, Arlington VA 22202-4302. Respondents should be aware that notwithstanding any other provision of law, no person shall be subject to a penalty for failing to comply with a collection of information if it does not display a currently valid OMB control number.

1. REPORT DATE <b>1998</b>		2. REPORT TYPE		3. DATES COVERED <b>00-00-1998 to 00-00-1998</b>	
4. TITLE AND SUBTITLE <b>A Dendritic Model of Coincidence Detection in the Avian Brainstem</b>				5a. CONTRACT NUMBER	
				5b. GRANT NUMBER	
				5c. PROGRAM ELEMENT NUMBER	
6. AUTHOR(S)				5d. PROJECT NUMBER	
				5e. TASK NUMBER	
				5f. WORK UNIT NUMBER	
7. PERFORMING ORGANIZATION NAME(S) AND ADDRESS(ES) <b>University of Maryland, Department of Electrical Engineering and Computer Engineering, Institute for Systems Research, College Park, MD, 20742</b>				8. PERFORMING ORGANIZATION REPORT NUMBER	
9. SPONSORING/MONITORING AGENCY NAME(S) AND ADDRESS(ES)				10. SPONSOR/MONITOR'S ACRONYM(S)	
				11. SPONSOR/MONITOR'S REPORT NUMBER(S)	
12. DISTRIBUTION/AVAILABILITY STATEMENT <b>Approved for public release; distribution unlimited</b>					
13. SUPPLEMENTARY NOTES					
14. ABSTRACT					
15. SUBJECT TERMS					
16. SECURITY CLASSIFICATION OF:			17. LIMITATION OF ABSTRACT <b>Same as Report (SAR)</b>	18. NUMBER OF PAGES <b>24</b>	19a. NAME OF RESPONSIBLE PERSON
a. REPORT <b>unclassified</b>	b. ABSTRACT <b>unclassified</b>	c. THIS PAGE <b>unclassified</b>			

# Introduction

Neural coincidence detection is essential in sound localization, which requires the computation of interaural time differences (ITDs) (for frequencies below a few kHz). This is performed by binaural cells in the avian Nucleus Laminaris (NL), and its mammalian homologue, the Medial Superior Olive (MSO).

A “coincidence detector” neuron should fire when inputs from two independent neural sources coincide (or almost coincide), but not when two inputs from the same neural source (almost) coincide. A neuron that sums its inputs linearly would not be able to distinguish between these two scenarios. Segregating the inputs on separate dendrites should avoid this problem: post-synaptic depolarization arising from a synaptic event is reduced if the dendrite has already been previously partially depolarized. This idea has been used by Agmon-Snir, Carr and Rinzel to model bipolar dendrites as interaural coincidence detectors in the avian auditory brainstem. This project is a more biophysical model, using the program NEURON, to explore the robustness of this mechanism and look for new mechanisms.

In addition, the active dendritic potassium channels (both low and high voltage activated), are incorporated. The high voltage activated channels (Kv1.2) vastly increase the cell's ability to phase lock at frequencies  $> 1$  kHz.

# Model Description

The model emulates a single neuron with an axon, soma, and a variable number of dendrites, each section with a variable number of equipotential compartments. All geometric, electrical, and channel parameters are adjustable, as are the number of synapses/dendrite (~30), the synaptic locations, and the distribution of synaptic locations. Channel types include potassium (high and low voltage activated [Kv1.1, 1.2], and delayed rectifier), sodium, and passive. Active channels have adjustable time and voltage parameters.

The stimulus is a pure tone of adjustable frequency, with variable binaural phase difference (or contralateral monaural stimulus with variable ipsilateral spontaneous activity). More complex stimuli can be easily introduced.

The synapses fire with conductance proportional to an alpha-function, with adjustable time constant, peak conductance, and reversal potential. The synapses fire as individual Poisson processes, with probability rate given by the half-wave rectified pure-tone, with adjustable amplitude and base spontaneous firing rate. The fast Kv3.1 channels of the pre-synaptic neurons are reflected in a short synaptic time constant.

The implementation uses the program NEURON and has an straightforward graphical user interface for controlling the parameters and running the model. NEURON provides a real-time display of data and analysis including the potential at various locations, the two stimuli, the synaptic firings, spike counters, period histograms of synaptic firings and the action potentials, and their vector strengths.

# NEURON Panels

Stimulus Frequency [Hz] 1000

Stimulus Phase Ipsi [Deg] 0

Stimulus Phase Contra [Deg] 0

Probability Rate [per ms] 3

Spontaneous Activity [0,1] 0.1

Action Pot. Threshold [mV] -35

Period Histogram bins 16

Cell-Wide Parameters ...

Synapse & Dendrite Parameters ...

Soma & Axon Parameters ...

Load Passive Dendrites

Load Active Dendrites

eNa [mV] 40

eK [mV] -80

eLeak [mV] -60

alpha0K LVA [/ms] 0.167

beta0K LVA [/ms] 0.02237

eta\_alphaK LVA [/mV] 0.00533

eta\_betaK LVA [/mV] -0.0617

vHalfK HVA [mV] -16

kK HVA [mV] 5.3

tauK HVA [ms] 10

Init (mV) -64

Init & Run

Stop

Continue til (ms) 250

Continue for (ms) 50

Single Step

t (ms) 250.05

Tstop (ms) 250

dt (ms) 0.0125

Points plotted/ms 20

Show Time Plots

Show Info Strips

SimulationControl

Coincidence Parameters

Use Binaural Stimulus

gMSyn Follows IDen

gKHvaBar Follows IDen

Primary Parameter Control

# of Primary Pairs 16

Parameter to vary:

stimfreq

First Value 4000

Last Value 125

Vary with Log Scale

Slave parameter to vary:

-- none --

Slave First Value 11.892

Slave Last Value 160

Vary with Log Scale

Secondary Parameter Control

Use Secondary in Parallel

# of Serial Pairs 1

Parameter to vary:

-- none --

First Value 0.0004

Last Value 0.064

Vary with Log Scale

Slave parameter to vary:

-- none --

Slave First Value 0

Slave Last Value 0

Vary with Log Scale

Length (Soma) [um] 15

Diameter (Soma) [um] 15

Ax. Resistivity (Soma) [ohm cm] 200

gK LVA\_max (Soma) [S/cm^2] 0

gK HVA\_max (Soma) [S/cm^2] 0

gLeak (Soma) [S/cm^2] 0.0006

gNa\_max (Soma) [S/cm^2] 0

gK\_max (Soma) [S/cm^2] 0

# of Compartments (Soma) 5

Length (Axon) [um] 100

Diameter (Axon) [um] 2

Ax. Resistivity (Axon) [ohm cm] 200

gLeak (Axon) [S/cm^2] 0.0006

gNa\_max (Axon) [S/cm^2] 3.2

gK\_max (Axon) [S/cm^2] 2.2

# of Compartments (Axon) 5

# Synapses/dendrite 30

Synapse tau [ms] 0.1

Synapse gmax [uS] 0.03

Synapse e [mV] -0

Synapse shutoff factor 20

Synapse center [0,1] 0.5

Synapse distribution [0,1] 1

# dendrites 2

Length [um] 33.636

Diameter [um] 4

Ax. Resistivity [ohm cm] 200

gL [S/cm^2] 0.0006

gK LVA\_max [S/cm^2] 0.95

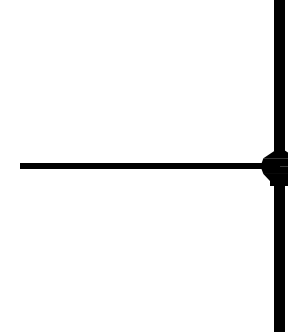
gK HVA\_max [S/cm^2] 0.034

# of Compartments 30

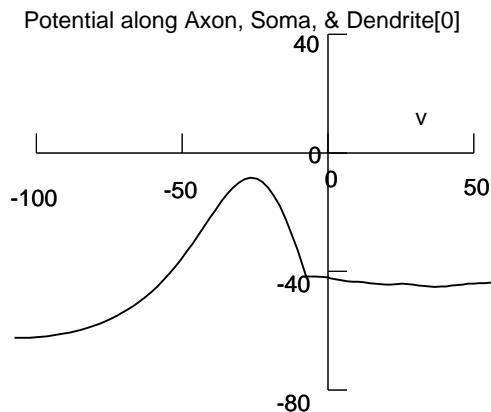
lambda [um] 288.68

# Spatial Geometry

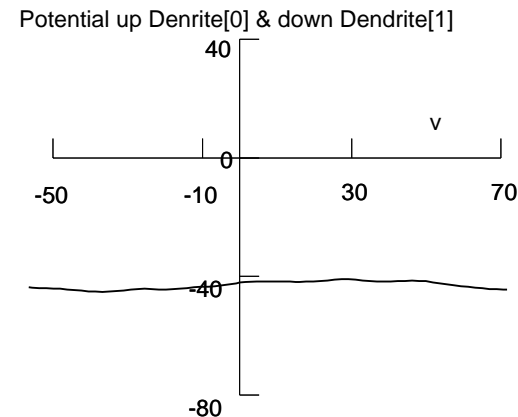
This typical model cell has 2 dendrites, each  $\sim 60 \mu\text{m}$  long and  $4 \mu\text{m}$  in diameter, a spherical soma of diameter  $15 \mu\text{m}$ , and an axon  $100 \mu\text{m}$  long and  $2 \mu\text{m}$  in diameter.



“Space plots” show the intracellular potential at every point in the cell (here at one instant in time).

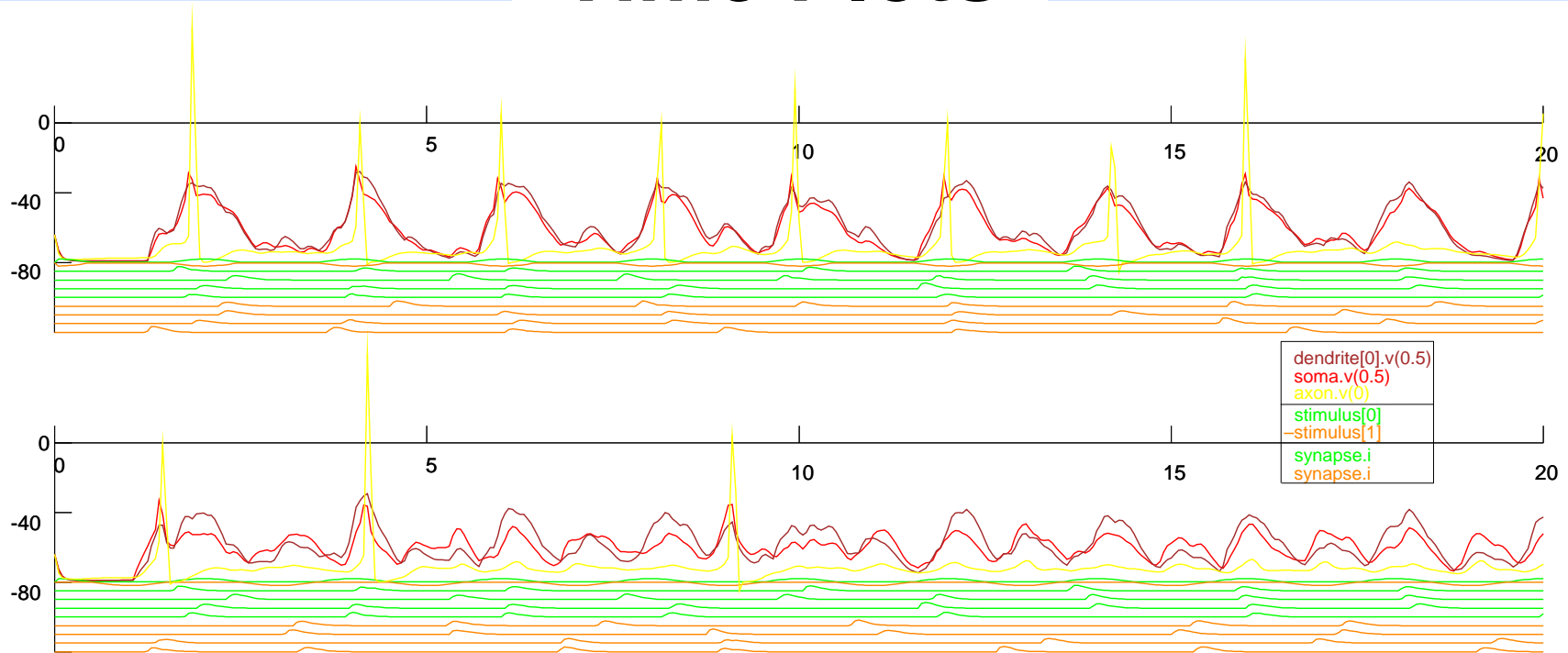


The potential along the curve:  
down the axon, through the soma,  
and down along one dendrite.



The potential along the curve:  
up one dendrite, through the soma,  
and down along the other dendrite.

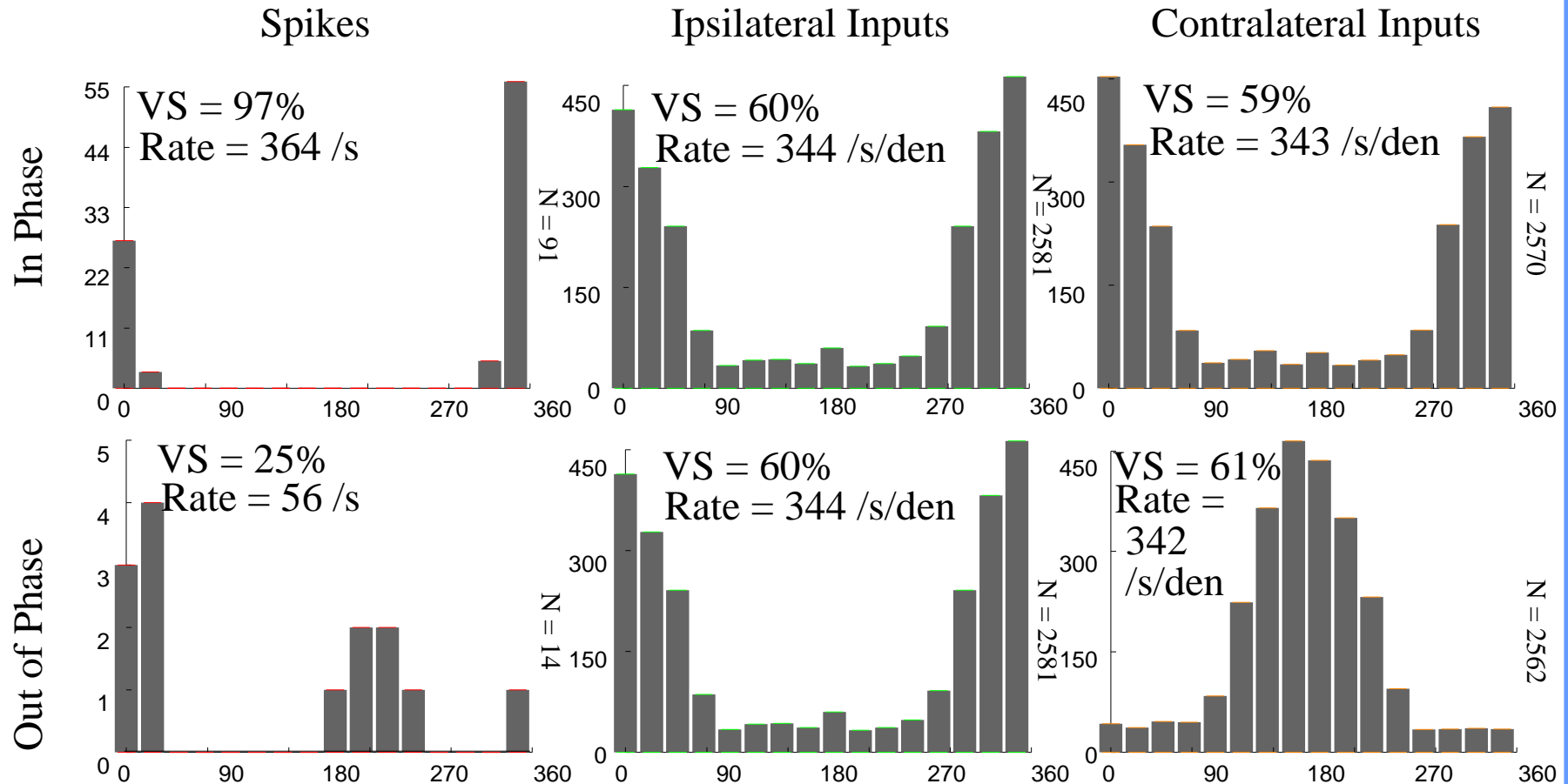
# Time Plots



Typical time plots (continuously updated). This pair of cells each receives the same stimulus probability distributions (at 500 Hz). The top cell receives its inputs binaurally in-phase, and the bottom out-of-phase.

The red curve tracks the intracellular potential at soma/axon boundary, the yellow at the axon tip, and the brown curve in one dendrite. Under are a pair of plots of the presynaptic probability distribution. The bottom 8 curves of each graph show actual synaptic currents (note the spread from the Poisson distribution).

# Period Stimulus Histograms



The same pair of cells (and stimulus), tracked for 250 ms. The vector strength (VS) is a measure of phase locking, ranging between 0 and 100%. The cell receiving in-phase stimulus increased its vector strength, the out-of-phase cell substantially reduced it. Note also the number of spikes in each case.

# Parameter Space & Dendritic Length

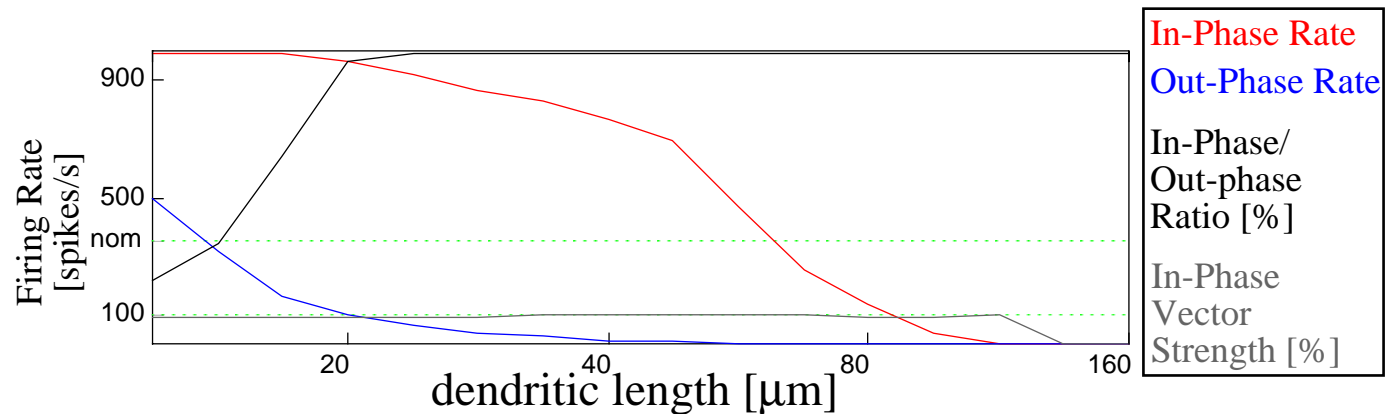
The dimensionality of the parameter space of this model is high. Only a small volume of the space of it is biologically relevant, but it is not immediately obvious where the relevant subspace lies.

The parameters fall into a few general categories: those whose values are experimentally known, those whose values are not. Some values fall in a particular range, and different ranging parameters may be correlated or not. Some parameters may be particularly relevant for certain species but not for others (e.g. the barn owl can detect ITDs up to 8 kHz, whereas the chicken can detect only up to 2 kHz).

To limit the search, we usually compare the performance of a pair of identical cells to identical stimuli, with one set of stimuli in-phase and the other out-of-phase.

As a first step, we pick “reasonable” values for all parameters, vary the dendritic length, compare firing rates and observe the vector strength of the in-phase case.

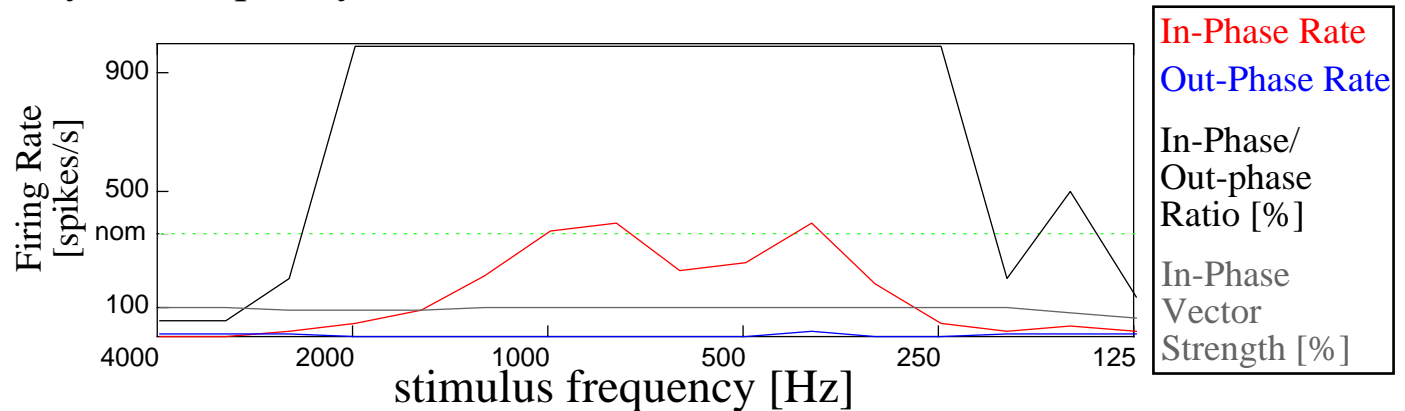
*The “nominal” firing rate of ~350 spikes/s is a typical best firing rate for an NL cell in chick.*



# Stimulus Frequency

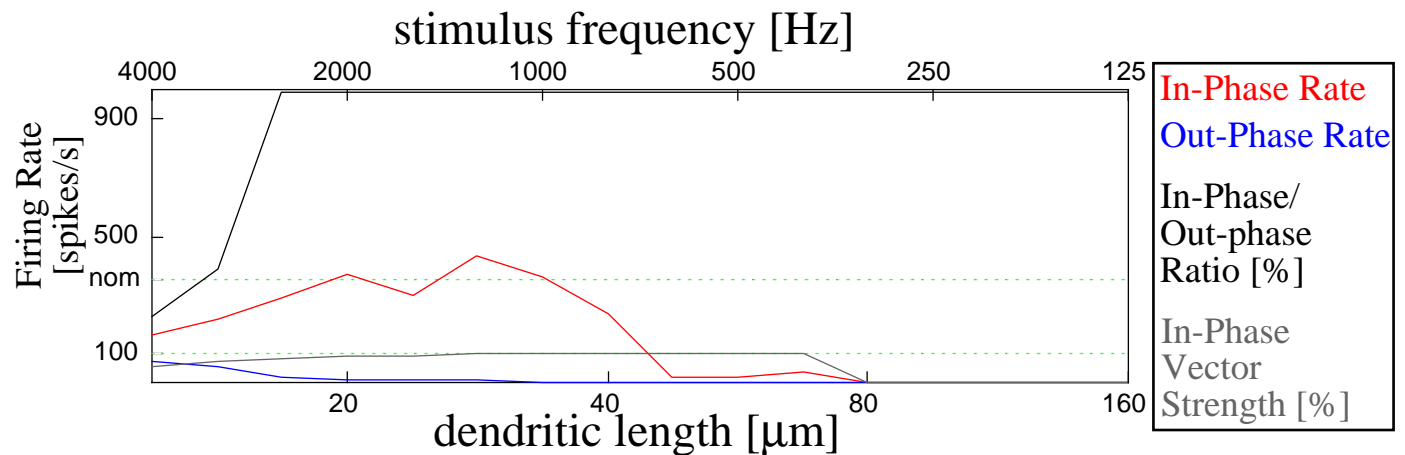
Next hold fixed the dendritic length at which the in-phase firing rate matches the “nominal rate,” and vary the frequency.

This cell responds best to frequencies between 300 and 1200 Hz.



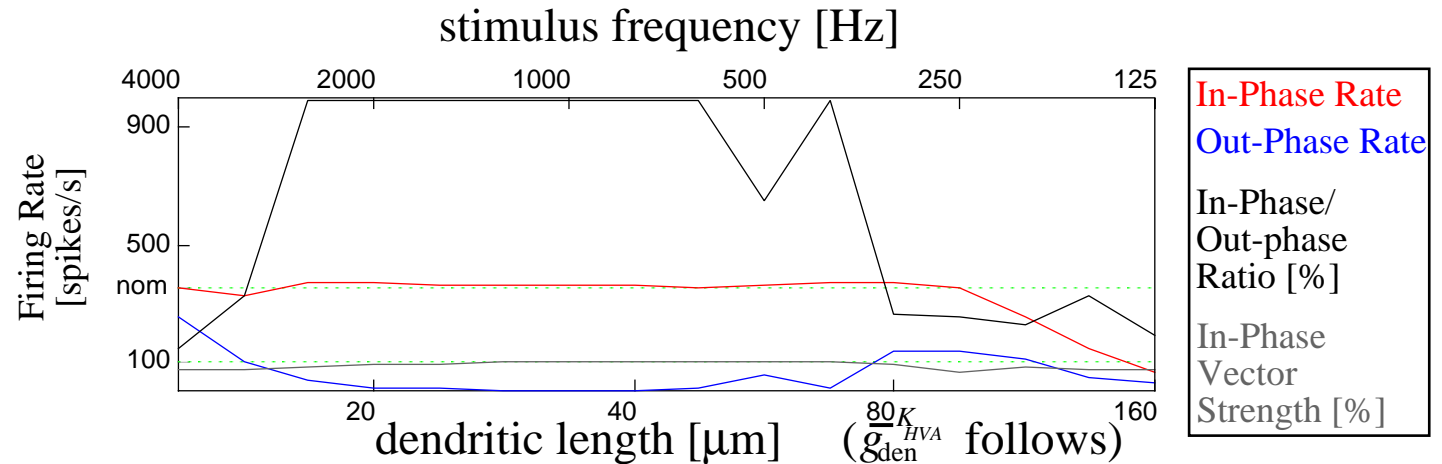
In the avian NL, the dendritic length varies (roughly) inversely with the best frequency of the cell. By directly covarying the stimulus frequency with the dendritic length, we can attempt to capture a central subspace of the entire parameter space.

With these parameters this class of cells does poorly below 800 Hz.

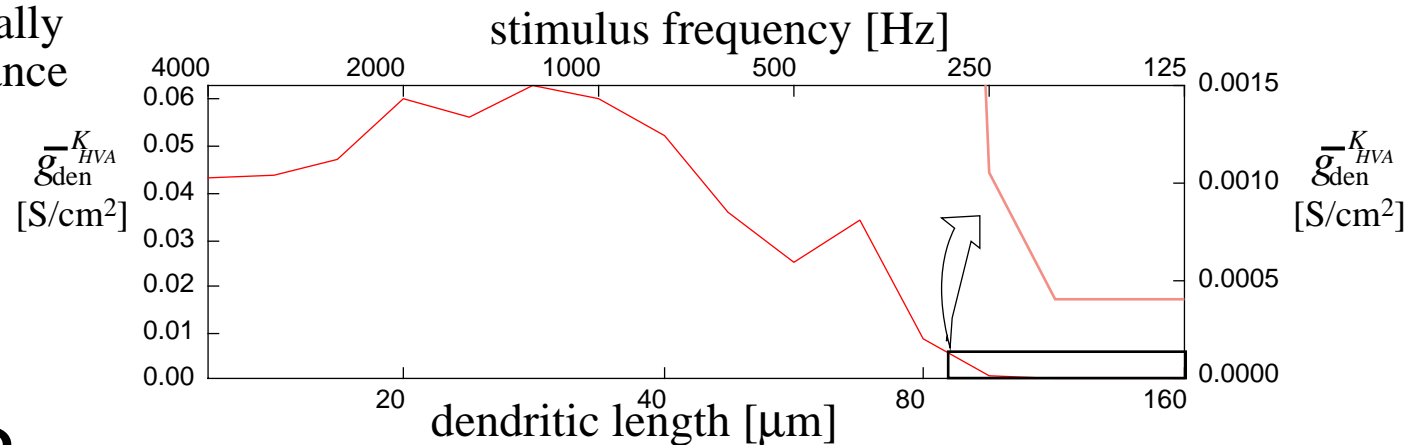


# Canonical Parameters

Covarying the stimulus frequency with the dendritic length gives us a curve that is relatively flat, but by covarying one additional parameter, the maximum dendritic conductance of the high voltage activated potassium channel ( $K_{HVA}$ ), we can get a rate curve that matches the nominal rate quite closely (at least at 250 Hz and above).



Computationally phenomenologically derived conductance function.

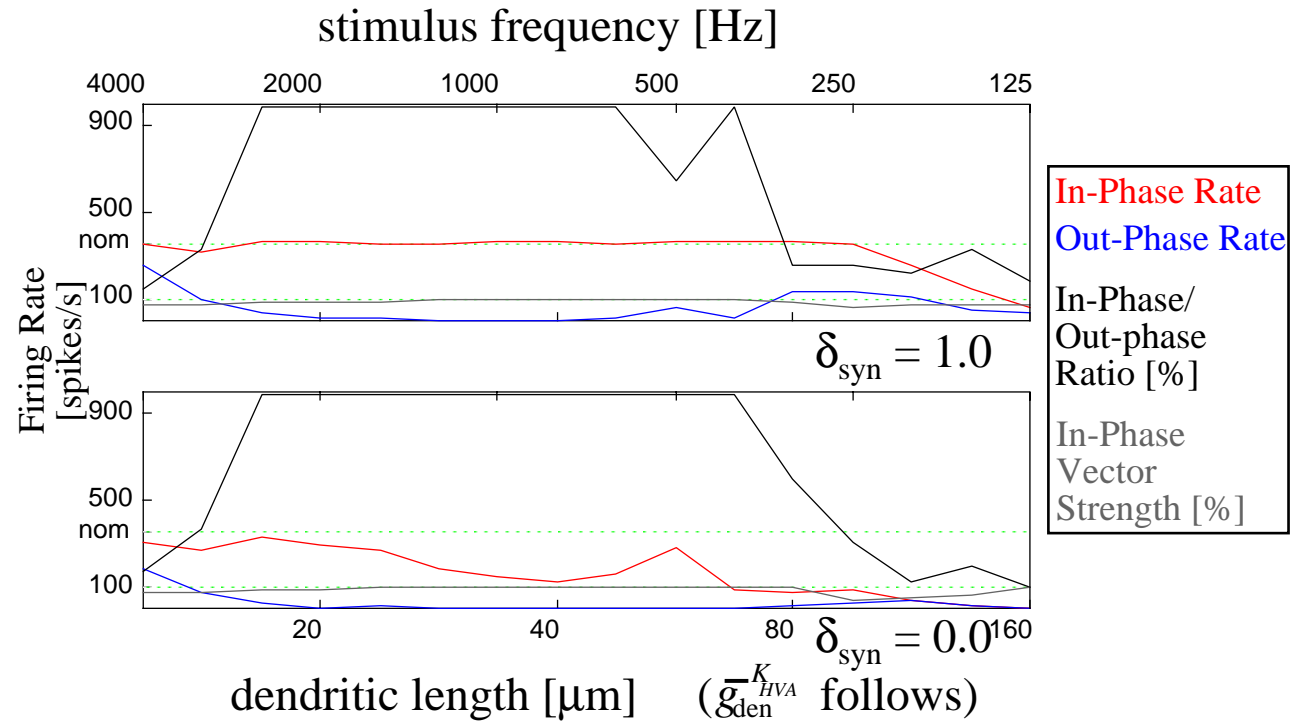


# Synaptic Distribution

Typically the synapses would be uniformly distributed along the dendrite. We can compare the base response to the response when all synapses are moved to the center of the dendrite.

The top figure is the base response, the bottom with all synapses at the center.

The effect is relatively small. The In-Phase rate is moderately reduced, worsening at large dendrites/low frequencies. The ratio of In-Phase rate to Out-Phase rate remains large in the same range.



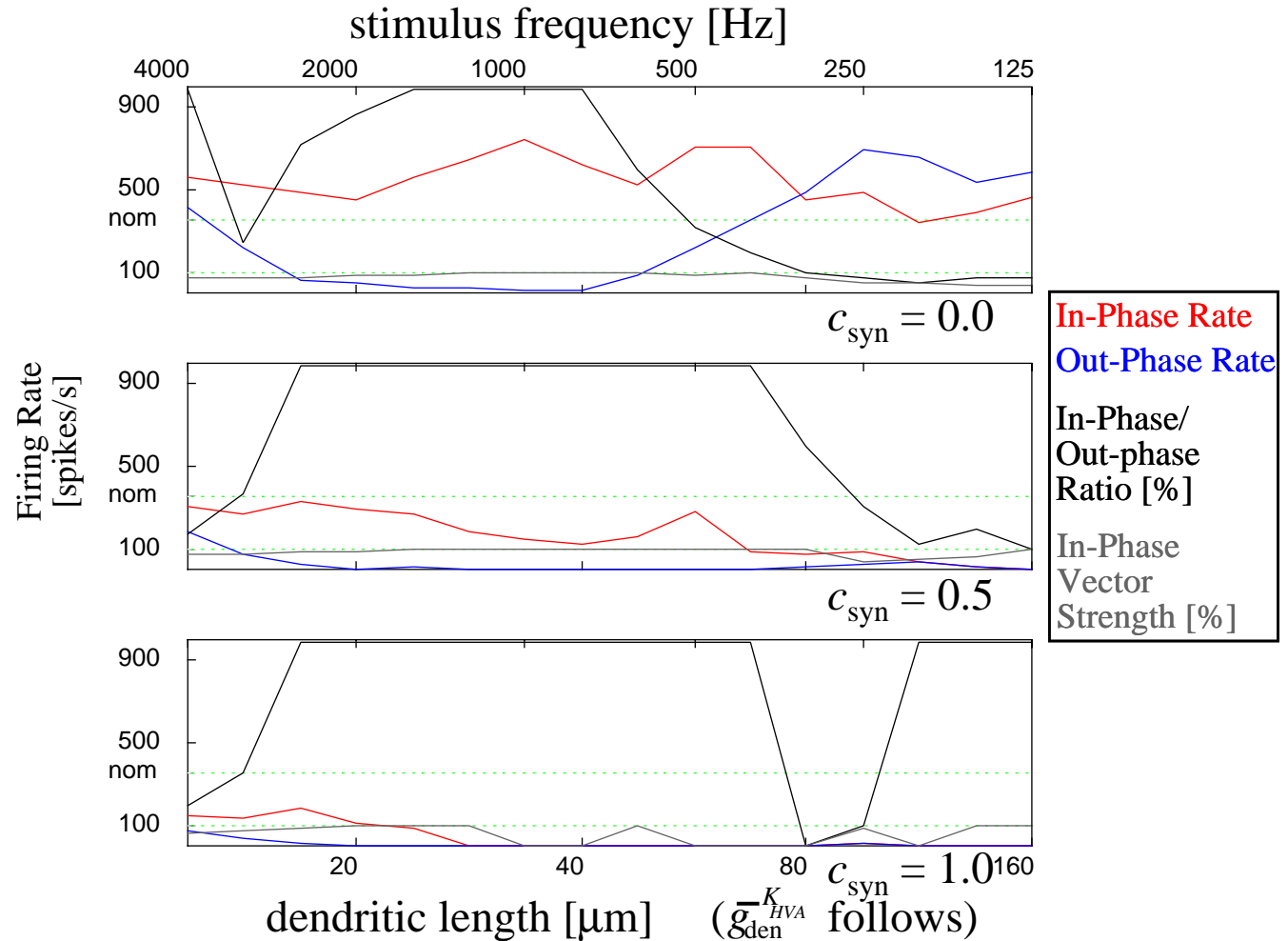
One might have expected the cell to perform better with all the synapses together, to reduce jitter from the differing travel times of the signals to the soma, but the dendrites are (electrotonically) relatively compact.

# Synaptic Location

We can also change the location of the concentrated synapses.

Here are the results from 3 cases: all synapses located at the dendrite base; halfway down the dendrite; at the dendrite tip.

At the base, the coincidence detector performs poorly for large dendrites/low frequencies, giving many false positives. The advantage of inputs adding sublinearly in the dendrites (which are much smaller compartments than the soma) is lost.

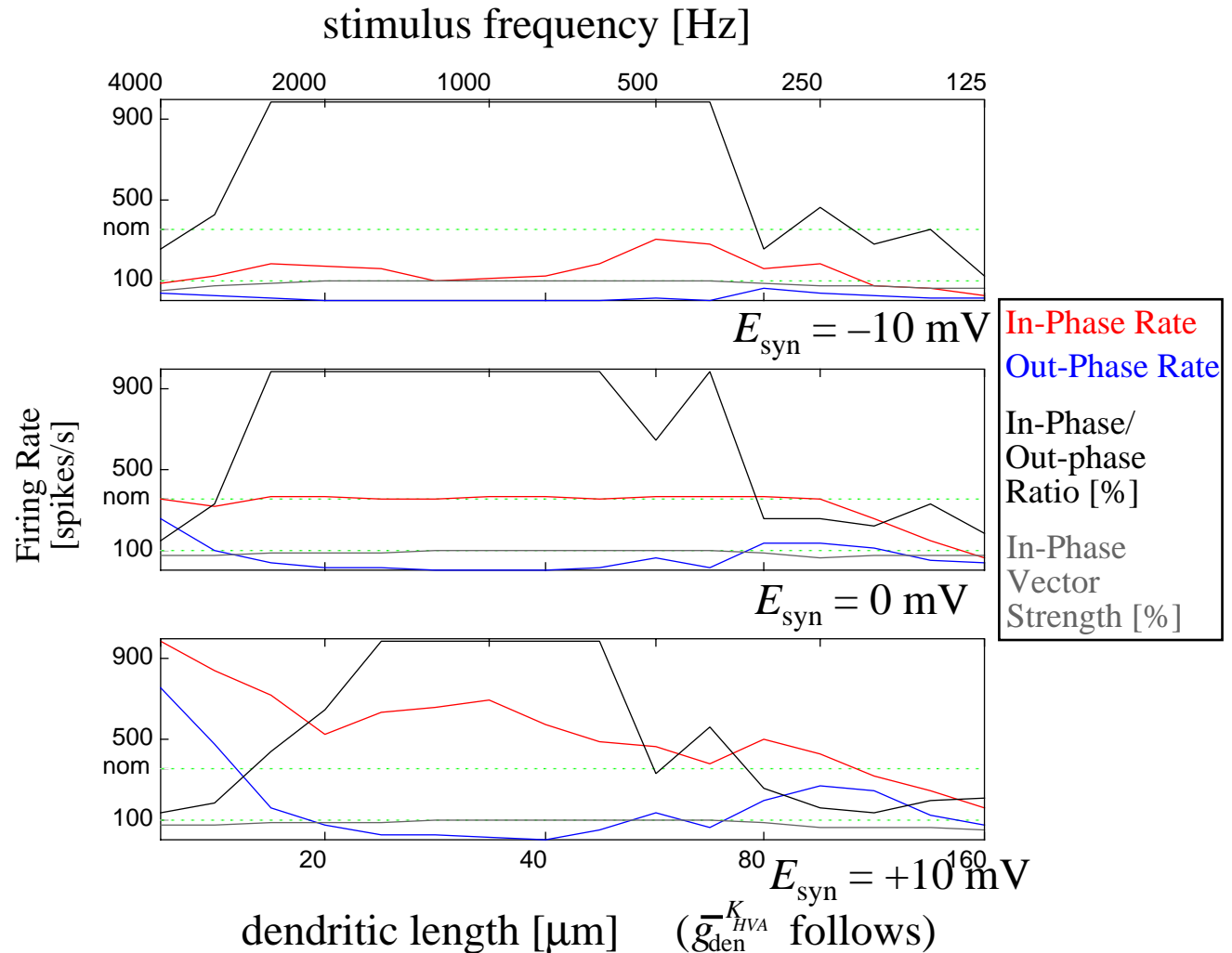


# Synaptic Reversal Potential

The benefit of sub-linear addition can also be seen by changing the synaptic reversal potential.

Here are the results from 3 cases: setting the reversal potential 10 mV too low, correctly, and 10 mV too high.

When the reversal potential is artificially raised, the sub-linear addition of the inputs is suppressed, and the coincidence detectors become effective over a smaller range of frequencies/lengths.

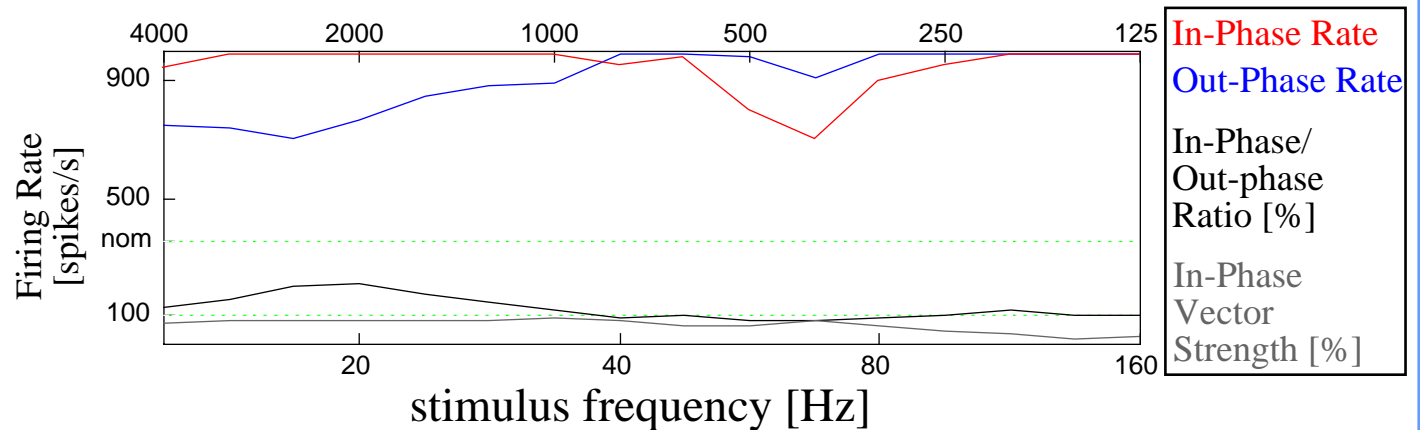


# Dendriteless Soma

This model supports the claim that dendrites are aiding in neural computation. How well does it perform compared to the same model without dendrites?

In the previous “Synaptic Location” panel, if the synapses are located at the dendrite/soma boundary, the performance is compromised. But the dendrites are still present and can still act as current sinks, which can increase coincidence detection ability.

In this trial the dendrites have been removed.



Firing rates rise dramatically, but they do so for both the In-Phase and Out-Phase cases. The ratio of the rates is near 1, indicating poor discrimination.

# Spontaneous Input

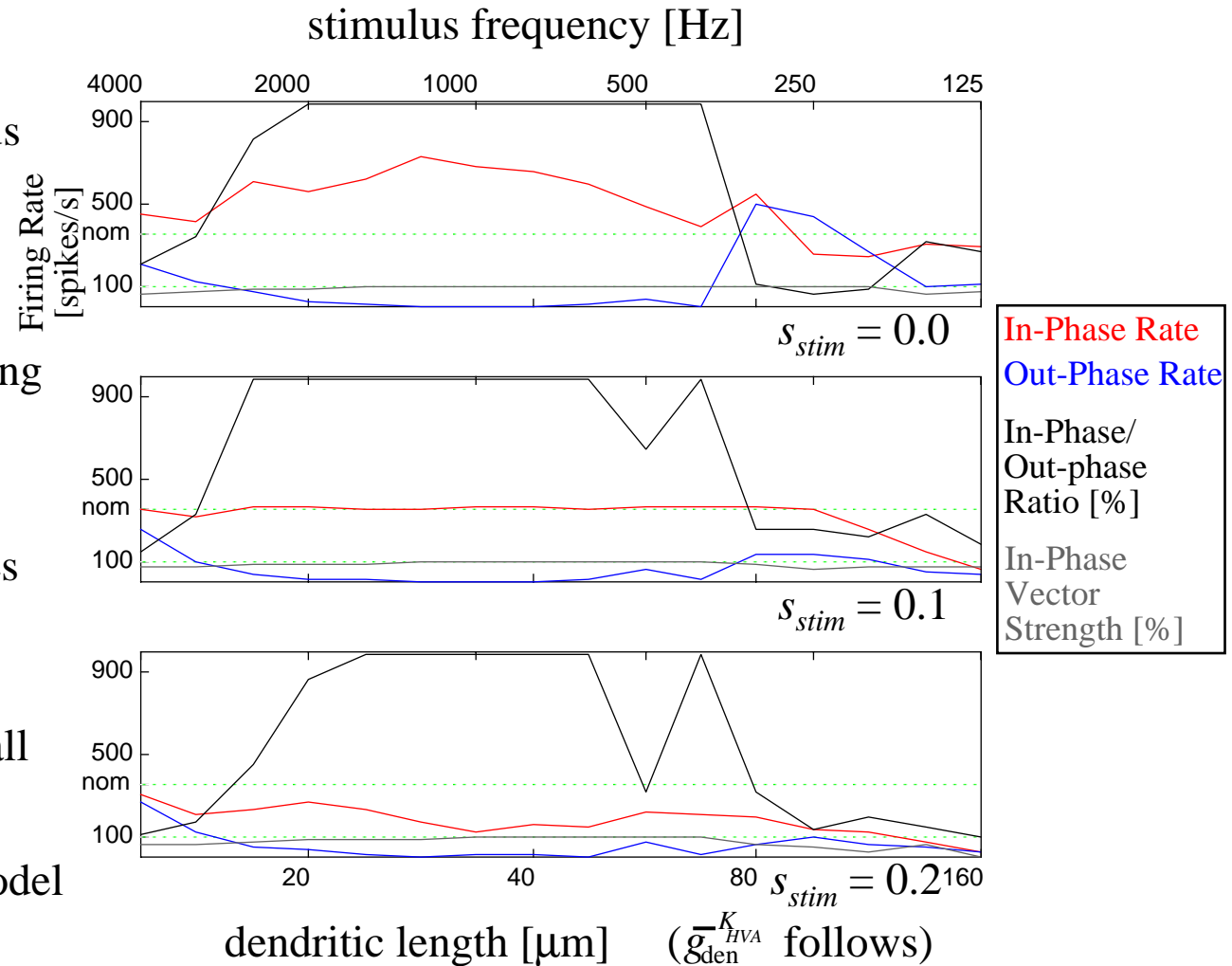
In this model, the input vector strength (VS) is determined by the spontaneous activity.

$s = 0$  gives no spontaneous activity. The half-wave rectified inputs have  $VS = 1/\sqrt{2} \approx 77\%$ .

$s = 0.1$  is our standard spontaneous activity, giving  $VS \approx 60\%$ .

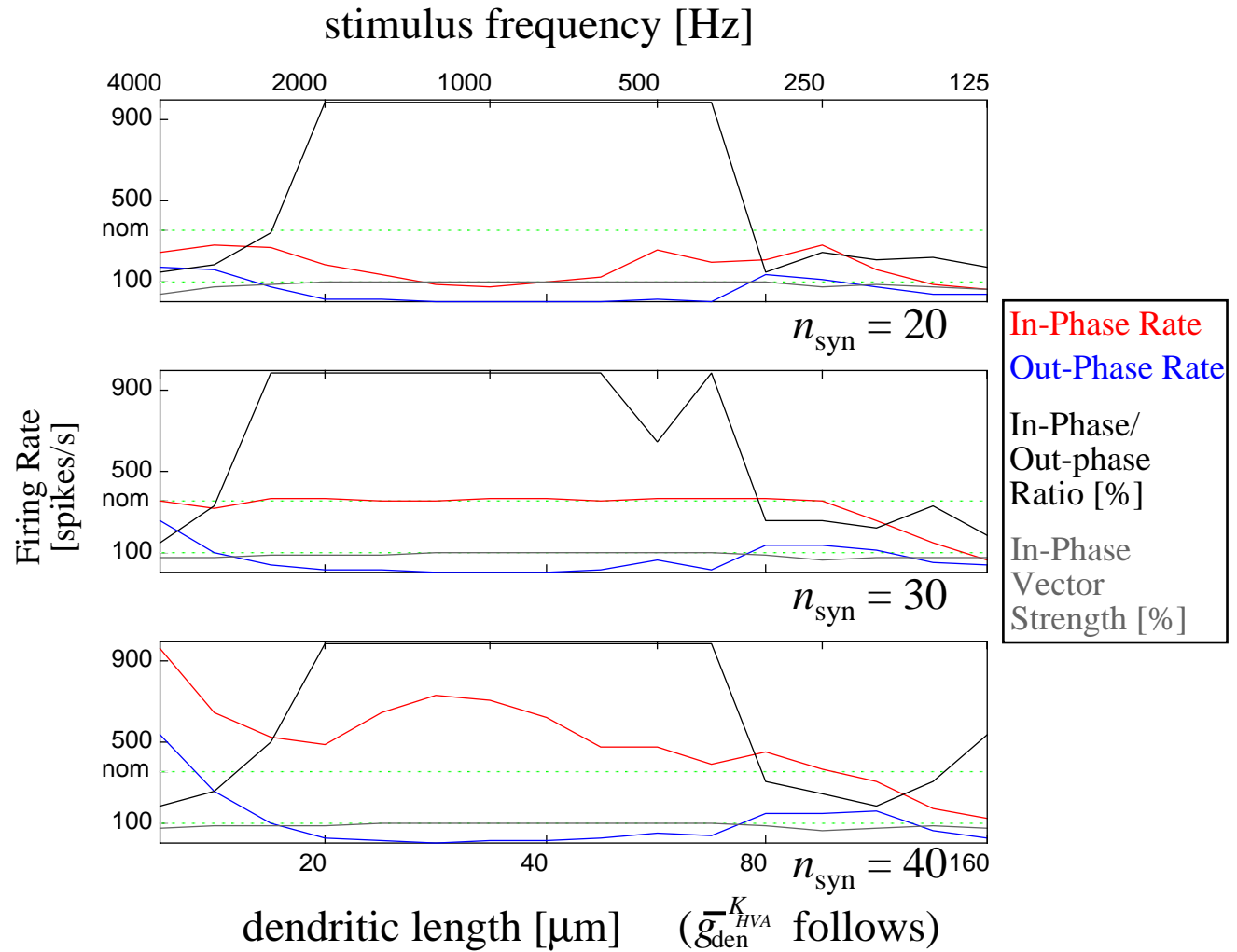
$s = 1.0$  gives  $VS = 0\%$ .

In the chick NL, VS varies from above 90% at the lowest frequencies, decreasing to below 50% above 1 kHz, and losing all phase locking by 2 kHz. This explains why the “canonical parameter” model outperforms the chick at high frequencies.



# Number of Synapses/Dendrite

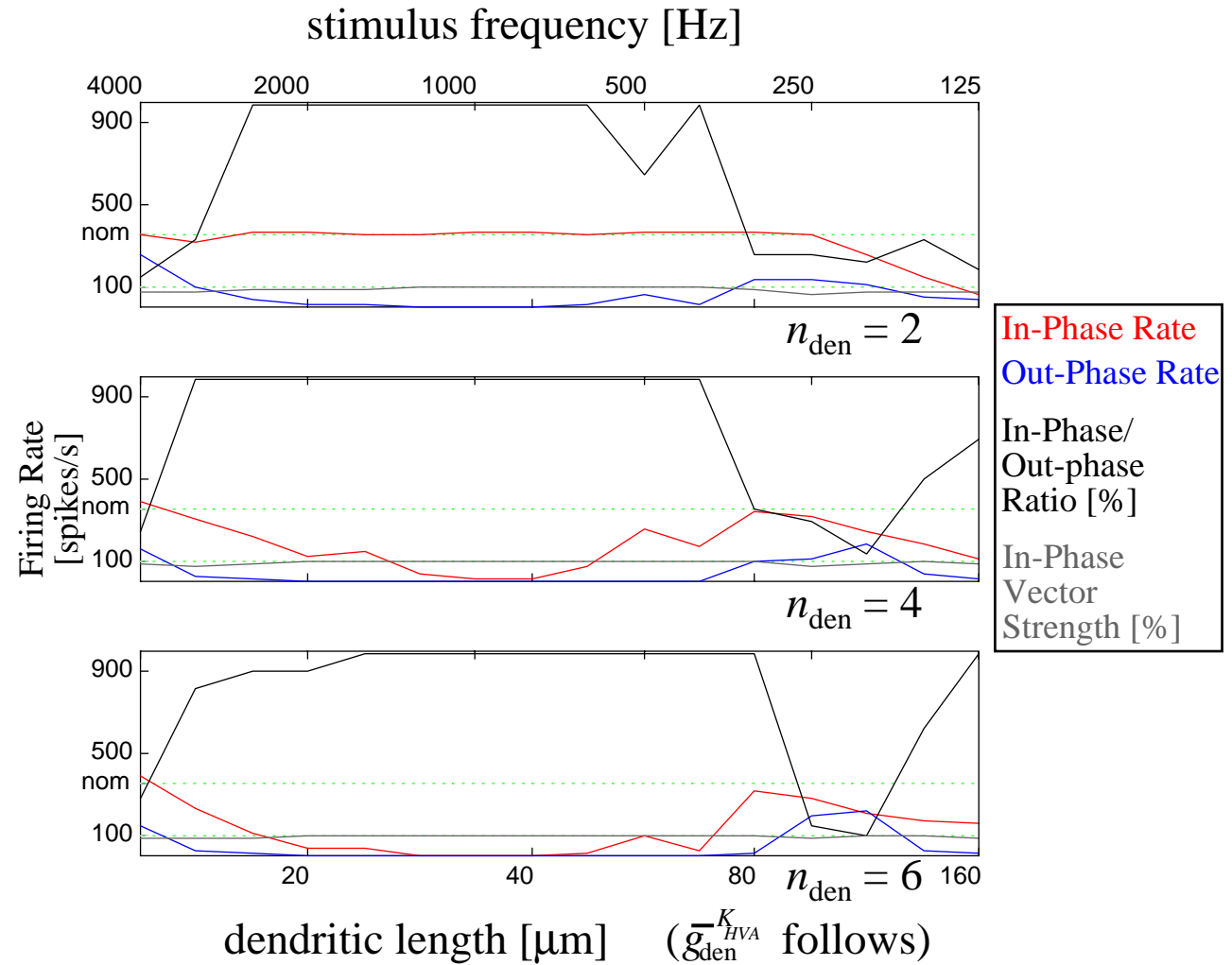
Coincidence detection is robust against changes in the number of synapses/dendrite.



# Number of Dendrites

Real NL Neurons have more dendrites at shorter lengths/higher frequencies.

In this model, more dendrites may enhance coincidence detection at high frequencies, but the evidence is murky.

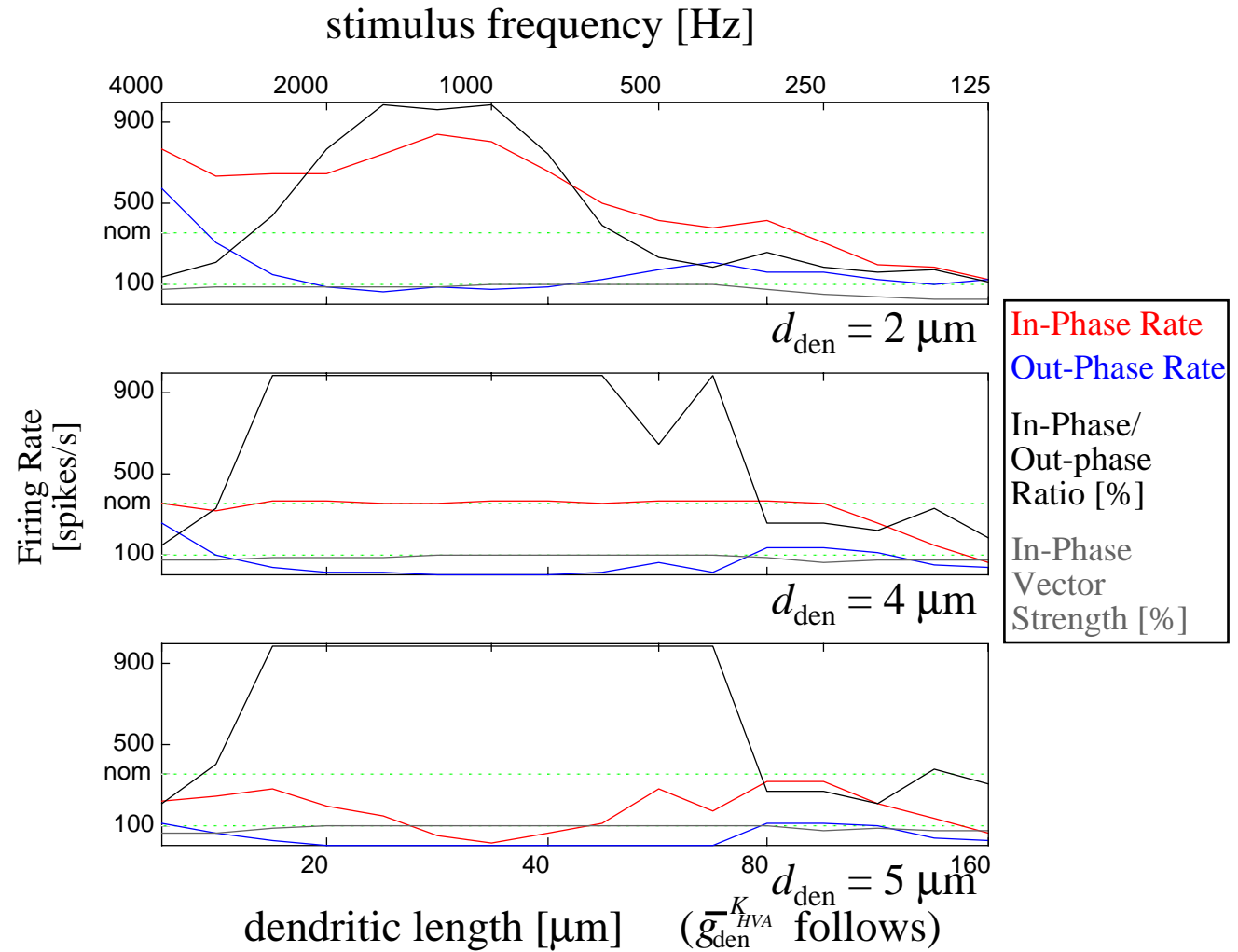


# Dendritic Diameter

Real NL Neurons vary in dendritic diameter from 2 to 4  $\mu\text{m}$ .

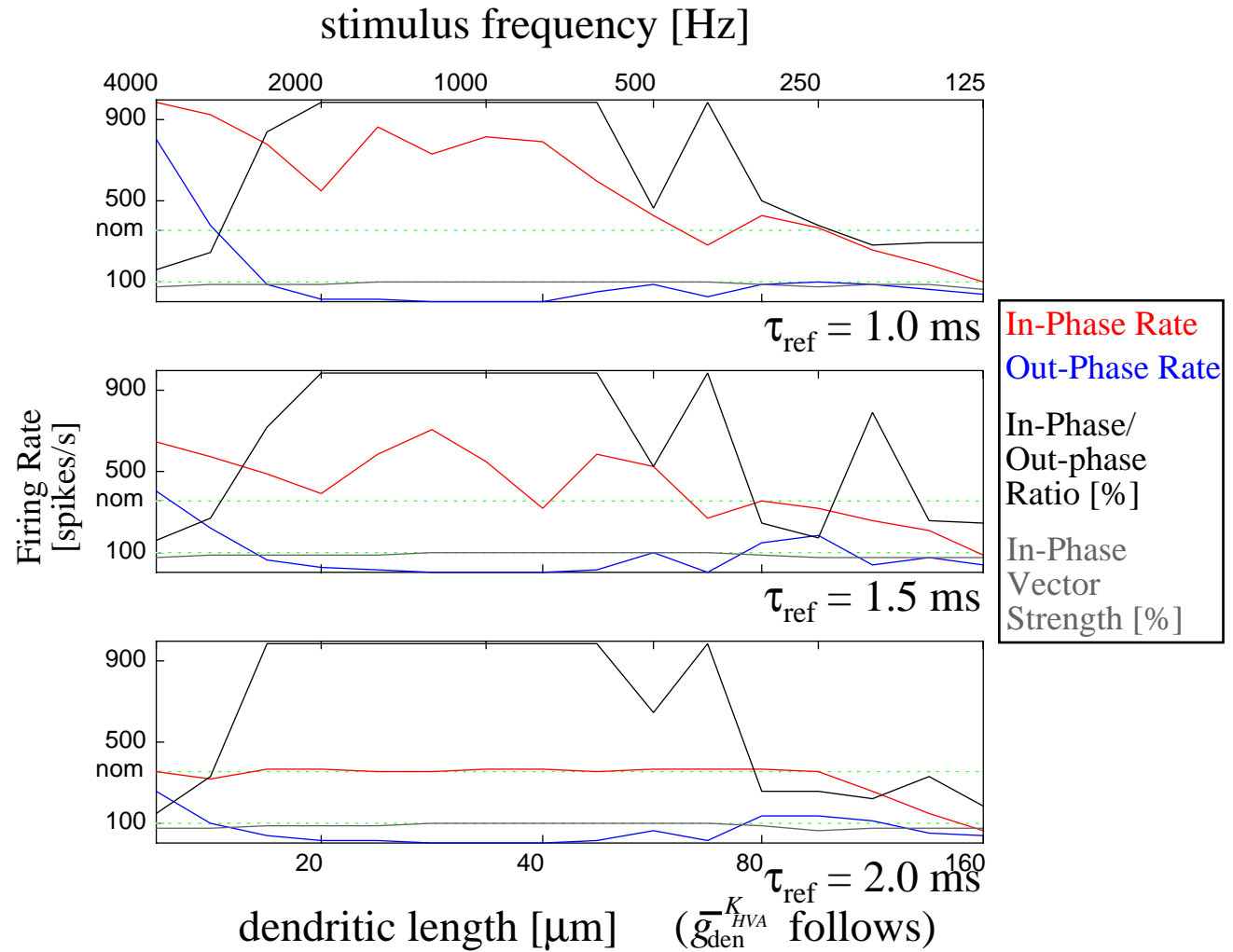
The major effects of this variation are changes in the electrotonic length and in the transmission coefficient to the soma.

This model indicates no benefit to having the thinner dendrite.



# Synaptic Refractoriness

The refractory time of the pre-synaptic inputs may be important for the low frequency/long dendrite case.

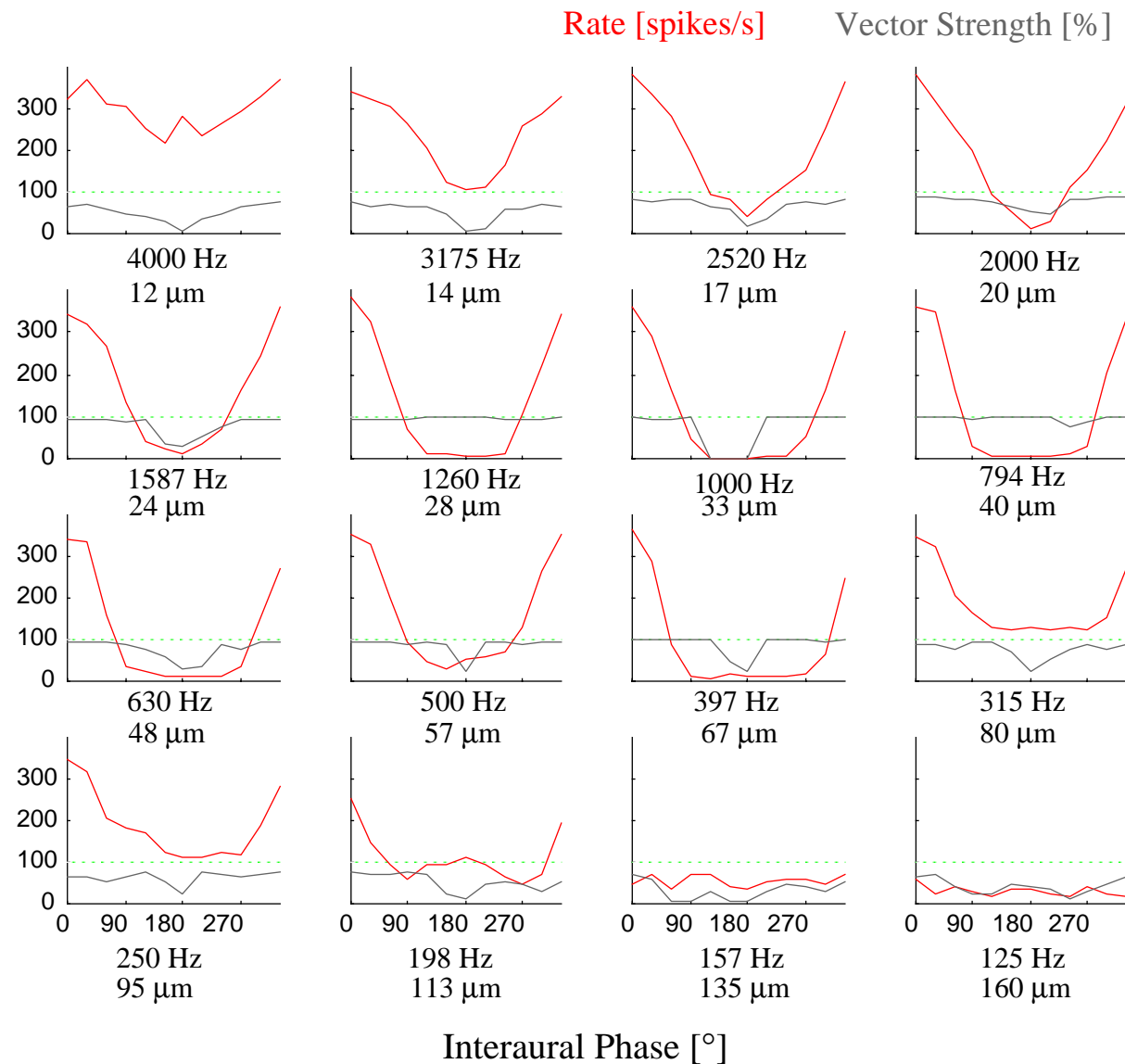


# Phase Locking

The NL contains arrays of coincidence detectors tuned to a wide range of phase differences (more than just  $0^\circ$  and  $180^\circ$ ).

Here are responses to a  $360^\circ$  range of phase difference.

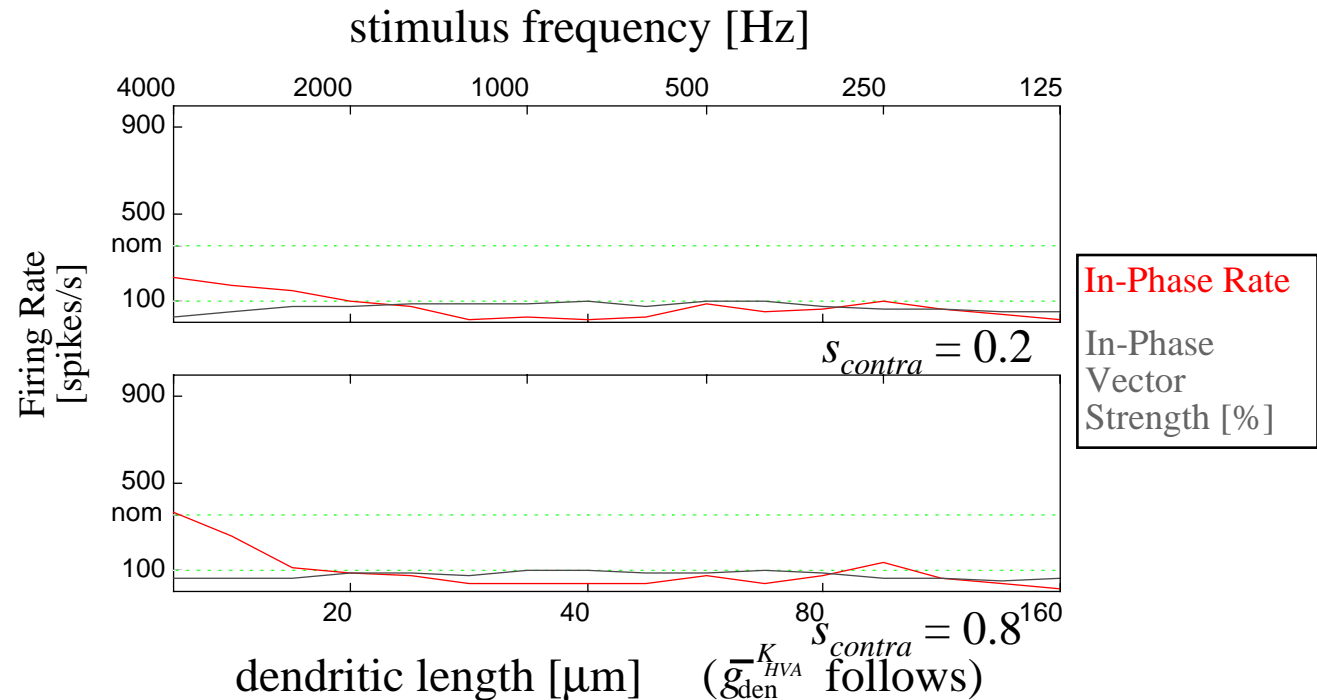
The firing rate and vector strength are both strong functions of phase difference, but the firing rate is more sharply tuned (and the vector strength is not reliable at low rates).



# Monaural Input

Real NL neurons also respond to periodic stimuli presented only in one ear. Presumably this is due to coincidence detection between the monaural stimulus one side and the spontaneous activity on the other side.

The model cell locks well to this monaural input, with a vector strength of near 1 for a broad range of inputs, though its firing rate is well below the nominal best rate for binaural input.



# Conclusions

- The model has parameter ranges that give behavior corresponding to the behavior of real NL neurons.
- The dendrites aid in the ability of the cell to perform coincidence detection, especially because of sublinear addition and dendritic current sinks.
- The high voltage activation potassium channels are important for coincidence detection at high frequencies (though roughly independent of the kinetics).
- Coincidence detection is robust against the number of incoming synapses.
- Regions in the parameter space have been identified for further investigation.
- The model predicts that vector strength is very robust (at fast firing rates), but is not as sharply tuned as firing rate as a function of phase difference.
- The model locks well to monaural stimulus.
- NEURON is an extremely effective environment for implementing a detailed biophysical model.

# Selected References

- “The Role of Dendrites in Auditory Coincidence Detection,” H. Agmon-Snir et al., *Nature* **393**, 268-272 (1998).
- “The NEURON Simulation Environment,” M. L. Hines and N. T. Carnevale, *Neural Computation* **9**, 1179-1209 (1997). See also <http://www.neuron.yale.edu>.
- “Organization and Development of Brain Stem Auditory Nuclei of the Chicken: Dendritic Gradients in Nucleus Laminaris,” D. J. Smith and E. W. Rubel, *J. Comp. Neur.* **186**, 213-240 (1979).
- “In Vitro Analysis of Optimal Stimuli for Phase-Locking and Time-Delayed Modulation of Firing in Avian Nucleus Laminaris Neurons,” A. D. Reyes, et al., *J. Neurosci.* **16**, 993-1007 (1996).
- “A Circuit for Detection of Interaural Time Differences in the Brain Stem of the Barn Owl,” C.E. Carr and M. Konishi, *J. Neurosci.* **10**, 3227-3246 (1990).
- “Two Voltage-Dependent  $K^+$  Conductances with Complementary Functions in Postsynaptic Integration at a Central Auditory Synapse,” H. M. Brew and I. D. Forsythe, *J. Neurosci.* **15**, 8011-8022 (1995).
- “The Differential Expression of Low-Threshold Sustained Potassium Current Contributes to the Distinct Firing Patterns in Embryonic Central Vestibular Neurons,” G. Gamkrelidze et al., *J. Neurosci.* **18**, 1449-1464 (1998).

# Abstract

The coincidence detector neurons in the auditory brainstem detect interaural time differences (ITDs). Inspired by a minimal biophysical model [Agmon-Snir et al, Nature **393**, 268-272 (1998)], we constructed a model using the NEURON environment. ITD coding was improved when the inputs from both ears were located on the bipolar dendrites and segregated over having both inputs on the soma. Thus the model behaves both like the in vivo coincidence detectors and the minimal model. The model has enabled us to explore features of the coincidence detector neurons unexplained by the simple biophysical model, including the effect of synapse location and multiple dendrites.